Mon. Not. R. Astron. Soc. **361,** 1243–1249 (2005) doi:10.1111/j.1365-2966.2005.09253.x

The double pulsar J0737–3039: testing the neutron star equation of state

Ph. Podsiadlowski,[1⋆] J. D. M. Dewi,[1,2] P. Lesaffre,[1,2] J. C. Miller,[1,3] W. G. Newton[4] and J. R. Stone[4,5,6]

[1]*Department of Astrophysics, University of Oxford, Oxford OX1 3RH*
[2]*Institute of Astronomy, Madingley Road, Cambridge CB3 0HA*
[3]*SISSA and INFN, via Beirut, 34014 Trieste, Italy*
[4]*Department of Physics, University of Oxford, Oxford OX1 3PU*
[5]*Department of Chemistry and Biochemistry, University of Maryland, College Park, MD 20742, USA*
[6]*Physics Division, ORNL, Oak Ridge, TN 37831, USA*

Accepted 2005 May 31. Received 2005 April 14

ABSTRACT

The double pulsar J0737–3039 has become an important astrophysical laboratory for testing fundamental physics. Here we demonstrate that the low measured mass of Pulsar B can be used to constrain the equation of state of neutron star matter *under the assumption* that it formed in an electron-capture supernova. We show that the observed orbital parameters as well as the likely evolutionary history of the system support such a hypothesis, and discuss future refinements that will improve the constraints this test may provide.

Key words: binaries: close – stars: evolution – stars: neutron – pulsars: general – pulsars: individual: J0737–3039.

1 INTRODUCTION

The discovery of the first double pulsar, J0737–3039 (Burgay et al. 2003; Lyne et al. 2004), consisting of two pulsars with spin periods of 22.7 ms (Pulsar A) and 2.77 s (Pulsar B) in a 2.4-h orbit, has opened up a new window for testing fundamental physics under extreme conditions: not only will the system soon allow some of the best tests of general relativity (Kramer et al. 2005), but also it is the first system where the physics of interacting magnetospheres from two pulsars can be studied (e.g. Arons et al. 2005). The orbit is decaying due to the loss of angular momentum by gravitational radiation, and the two neutron stars are expected to merge in only ∼85 Myr, a much shorter time than in any other double neutron star system.

One of the other interesting characteristics of J0737–3039 is that the mass of the second neutron star to be formed (Pulsar B) is the lowest reliably measured mass for any neutron star to date: 1.249 ± 0.001 $M_\odot$ (Kramer et al. 2005). Such a low mass may be an indication that the neutron star did not form in a standard iron core collapse supernova (SN) but in an electron-capture SN (Nomoto 1984; Podsiadlowski et al. 2004).[1] These occur for ONeMg white dwarfs when the core density reaches a critical value at which electron captures (e-captures) on to Mg (and subsequently Ne) start, causing a loss of hydrostatic support in the core and triggering its collapse. One of the key aspects of an e-capture SN is that the collapse takes places when the core density reaches a well-defined critical value ($\simeq 4.5 \times 10^9$ g cm^{-3}), which in turn occurs when the ONeMg core has grown to a well-defined critical mass ($\simeq 1.37$ $M_\odot$; see Section 3). Therefore, if Pulsar B indeed formed in an e-capture SN, this would be the first instance for which the gravitational masses of the pre-collapse core and the post-collapse neutron star could both be determined; the former from a *theoretical* estimate of the critical mass for an e-capture SN, and the latter directly from the *observed* orbital parameters. Along with the pre-collapse gravitational mass, the corresponding baryon number can also be calculated. Since the loss of material during the formation of the neutron star is expected to be extremely small in this scenario (see Section 3), this is also a good approximation to the baryon number of the neutron star. The purpose of this paper is to demonstrate that both the observed orbital parameters of the system (in particular the low eccentricity) and the most likely evolutionary history of the system favour the formation of Pulsar B in an e-capture SN, and that comparison of its gravitational mass with the estimate obtained for the baryon number enables useful constraints to be placed on the neutron star equation of state (EoS).[2]

In Section 2, we review the two most likely evolutionary channels that lead to systems like the double pulsar and show how this discussion supports the key assumption of Pulsar B having been

⋆E-mail: podsi@astro.ox.ac.uk

[1] Note, however, that it is not entirely clear that electron-capture SNe necessarily produce the lowest remnant masses, since iron cores with masses as low as 1.15 $M_\odot$ may be unstable to collapse (see the discussion in Woosley, Heger & Weaver 2002).

[2] A different test of the EoS of neutron star matter can be derived from measuring the moment of inertia of Pulsar A from the effects of spin–orbit coupling, as proposed by Morrison et al. (2004).

formed in an e-capture SN. In Section 3, we provide a theoretical estimate for the pre-collapse core mass (with an estimate of the uncertainties), and in Section 4 we demonstrate how the properties of the system can be used to constrain the neutron star EoS.

2 THE EVOLUTIONARY HISTORY OF J0737–3039

There are two major evolutionary channels to form double neutron stars like the double pulsar, which we will refer to in this paper as the standard channel (e.g. Bhattacharya & van den Heuvel 1991) and the double-core channel (e.g. Brown 1995), respectively. In the standard channel (see the left panel in Fig. 1), J0737–3039 originates from a massive binary in which the more massive star transfers its envelope to its companion star via stable Roche lobe overflow before it collapses in a SN explosion to form the first neutron star. If the SN explosion does not disrupt the system, the binary now consists of a neutron star and a massive main-sequence star, and the system will evolve into a high-mass X-ray binary (observationally it will initially look like a Be X-ray binary). As the secondary evolves, there will be a point at which it will fill its Roche lobe and start to transfer matter to the neutron star. Because of the large mass ratio of the system, this mass transfer is unstable and leads to a common-envelope (CE) and spiral-in phase, in which the neutron star spirals towards the centre of the massive companion inside the companion's envelope. Provided that the CE phase does not lead to the complete merger of the two components and that the CE is ejected, the system evolves into a very close binary containing the helium core of the secondary and the neutron star. Depending on the mass of the helium star and the period of the system, another phase of mass transfer may occur, where the neutron star is spun up and becomes a fast 'recycled' pulsar. Eventually, the helium star collapses to form the second neutron star in the system.

In the double-core channel (see the right panel in Fig. 1), the binary components are very close in mass initially (within 5–10 per cent), and the orbit is relatively wide, so that the primary only fills its Roche lobe after it has completed helium core burning (so-called Case C mass transfer) and has developed a CO core. At this stage, the secondary has already completed its hydrogen core burning phase and has evolved off the main sequence. Because of the high mass transfer rate, the accreting star expands to fill and ultimately overflow its Roche lobe, and the system is again expected to enter into a CE phase; but, in this case, the CE is formed from the *combined* envelopes of both stars. Inside the CE, there are the cores of the two stars, the more evolved one with a CO core and the less evolved He core of the secondary. The cores spiral-in inside the joint envelope until the envelope is ejected, leaving a very close binary consisting of the two evolved cores. The CO core soon collapses to form the first neutron star, leaving a binary consisting of a neutron star and a helium star. The further evolution is almost identical to the evolution in the standard scenario.

Because of the constraints on the initial mass ratio and the orbital separation, the double-core channel is expected to have a lower occurrence rate than the standard channel (by a factor of 2–10; Dewi, Podsiadlowski & Sena, in preparation).[3]

[3] However, if the spiral-in of a neutron star in a massive envelope always leads to hypercritical accretion on to the neutron star and its conversion into a black hole, as argued e.g. by Brown (1995), the double-core channel would be the only one of these two channels that could produce double neutron star systems (also see Chevalier 1993).

The formation of J0737–3039 via the standard channel has been studied by Dewi & van den Heuvel (2004) and Willems & Kalogera (2004); both studies concluded that this system must have originated from a close helium star–neutron star (HeS–NS) binary where the system underwent mass transfer during the helium star phase, spinning up the first-born neutron star in the process. Because the final stages of evolution in the standard and the double-core channel are essentially the same, i.e. the HeS–NS phase, the following discussion, which assumes the standard channel, also applies to the double-core channel.

For different reasons, Dewi & van den Heuvel (2004) and Willems & Kalogera (2004) found a similar pre-SN mass of the helium star progenitor of J0737–3039. Willems & Kalogera (2004) took the threshold helium star mass for the formation of a neutron star to be 2.1 $M_\odot$ (Habets 1986) as the lower limit. However, one should note that after the mass-transfer phase, the immediate pre-SN mass can be as low as the Chandrasekhar mass ($\sim$1.4 $M_\odot$). Dewi & van den Heuvel (2004) used 2.3 $M_\odot$ as the minimum possible helium star mass at the time of the explosion, based on the assumption that lower-mass helium stars experience a further CE phase at the end of their evolution (Dewi et al. 2002; Dewi & Pols 2003). This lower limit on the pre-SN mass then required a minimum kick velocity of 70 km s^{-1}, since the SN mass loss on its own would produce a much larger post-SN eccentricity than is consistent with the present orbital parameters of J0737–3039.

However, the assumption of the occurrence of another CE phase in a lower-mass helium star is still an open question. A recent population synthesis study of the formation of double neutron stars (Dewi, Pols & van den Heuvel, in preparation) suggests that, particularly to explain the formation of J0737–3039, it is more likely that this CE phase does not occur. In this case, the final pre-SN mass can be much less than 2.3 $M_\odot$, indeed it can be as low as $\simeq$1.4 $M_\odot$, and no SN kick is required to compensate for the mass loss; in particular it allows for the possibility that the SN was symmetric (Dewi & van den Heuvel 2005), strongly favouring an e-capture SN for the second SN.

2.1 An electron-capture SN to form Pulsar B?

The eccentricity of the double pulsar binary ($e \simeq 0.088$ at present, most likely 0.11–0.12 immediately after the second SN; e.g. Burgay et al. 2003) is surprisingly low, much lower than one would expect if the system received a large SN kick in the second SN that formed Pulsar B. Indeed, such a low eccentricity can be most easily explained by a symmetric second SN with a moderate amount of mass loss in the SN. In this case, the eccentricity is given by $e = \Delta M/(M_{\rm A} + M_{\rm B})$, where ΔM is the mass lost in the SN, and $M_{\rm A}$ and $M_{\rm B}$ are the present masses of Pulsars A and B, respectively. Taking $M_{\rm A} = 1.338$ $M_\odot$ and $M_{\rm B} = 1.249$ (Kramer et al. 2005) and assuming a post-SN eccentricity $e_0 = 0.12$ then yield a pre-SN mass of the helium star of $\simeq$1.56 $M_\odot$. Such low-mass pre-SN helium stars typically form from HeS–NS binaries with initial helium stars of less than $\sim$3 $M_\odot$ (see Dewi et al. 2002; Ivanova et al. 2003). This includes the mass range where helium stars are expected to end their evolution in an e-capture SN (Nomoto 1984). This is also consistent with the speculation by Podsiadlowski et al. (2004) that e-capture SNe may not produce large SN kicks since the explosion may proceed on a time-scale that is much shorter than the time-scale on which the instabilities that produce large kicks can develop; this suggestion has received some theoretical support from recent core-collapse calculations (Scheck et al. 2004; Janka, private communication). Since in any *simple* accretion model one

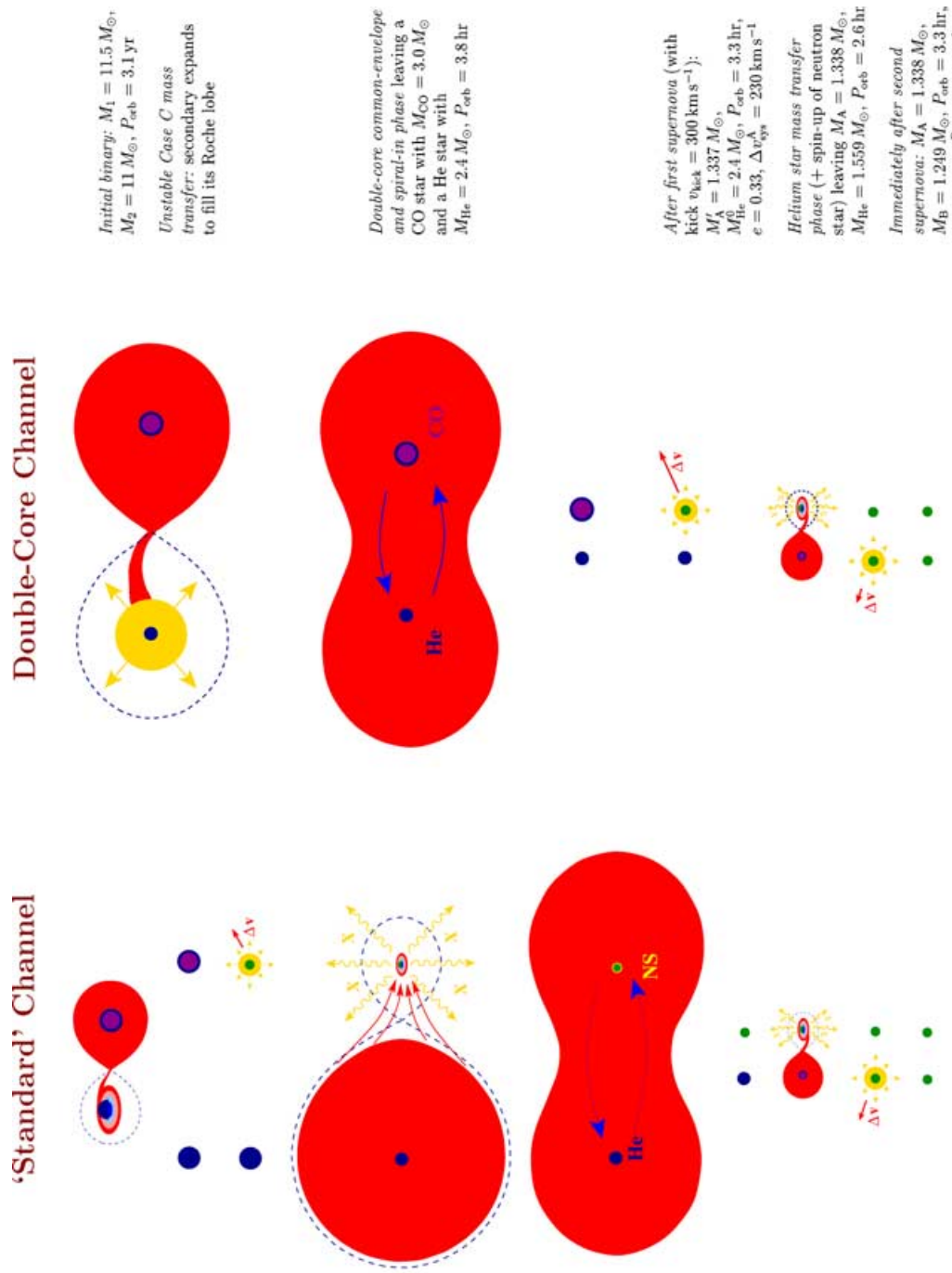

Figure 1. Schematic diagrams illustrating the evolutionary history producing systems like the double pulsar in the two main evolutionary channels. The final orbital parameters (10^8 yr after the second SN) are identical to those of J0737–3039. The double-core channel is expected to be less common than the standard channel by a factor of 2–10. Note the similarity in the final evolutionary stages, but the difference in kick-induced system velocities (∼40 and ∼230 km s $^{-1}$) in the two channels.

would expect that the spin of Pulsar A would become aligned with the orbital momentum axis and since this orientation is not affected by a symmetric SN, this may make the testable prediction that the post-SN misalignment angle between the spin of Pulsar A and the orbital axis should be relatively small. This may indeed account for the surprising stability of the pulse shape of Pulsar A (Manchester et al. 2005).

2.2 The second SN kick and the space velocity of J0737–3039

A low SN kick velocity, as suggested by the low eccentricity, would typically also imply that the binary system should only have received a relatively small additional kick in the second SN and that the system space velocity relative to the local standard of rest would not be much affected by it. Indeed, the space velocity of J0737–3039 may provide an important constraint on its evolutionary history. Unfortunately, the situation regarding the value of this quantity is at present somewhat confusing. Using interstellar scintillation to measure the transverse space velocity of the system, Ransom et al. (2004) determined a large system velocity of at least $140\,\mathrm{km\,s^{-1}}$. Subsequently, Coles et al. (2005) showed that the dispersion across the field was highly variable reducing the estimate of the scintillation velocity to a value as low as $66\,\mathrm{km\,s^{-1}}$ and possibly even lower, since this value does not account for the motion of the Earth. More recently, Kramer et al. (2005) argued that the present limits on the proper motion of the system suggest a low transverse velocity of less than $30\,\mathrm{km\,s^{-1}}$, which would imply that it is statistically unlikely that the system received a large kick in the second SN. On the basis of the original high estimate of the space velocity, Ransom et al. (2004) and Willems, Kalogera & Henninger (2004) concluded that the system should have received a large kick in the second SN. However, they only considered the standard scenario in which the system is still fairly wide at the time of the first SN; this implies that it cannot receive a large kick in the first SN and remain bound (see Fig. 1). In contrast, in the double-core scenario, where the system is already very tight at the time of the first SN, the system is expected to receive a large systemic kick from the first SN (of the order of 150–400 $\mathrm{km\,s^{-1}}$: see Fig. 1 and Dewi et al. 2005), and hence no additional kick from the second SN would be required. As far as testing the EoS is concerned, it is not important whether the system velocity is low or high, since both can be understood within the framework of either of the two channels and a small second kick. In particular, we note how similar the final phases are in the two channels. A resolution of the issue of the system's space velocity could, however, provide a powerful discriminant between the standard channel and the double-core channel.

3 ELECTRON-CAPTURE SUPERNOVAE

An e-capture SN occurs when the central density of an ONeMg core reaches the threshold value $\rho_{\rm th}$ for electron captures on ^{24}Mg. This decreases the electron pressure and the electron fraction $Y_{\rm e}$, lowering the Chandrasekhar mass and triggering the collapse of the core (Miyaji et al. 1980).

In order to estimate the uncertainties in the critical mass of the collapsing core, we performed a series of stellar structure calculations assuming non-rotating cores in hydrostatic equilibrium with a prescribed central density, homogeneous composition and a specified thermal profile. Since the heat released by the e-captures gives rise to a convective core, we adopted an isentropic thermal profile.

As our reference model, we adopted the composition given by Gutiérrez et al. (1996) with $X(^{16}\mathrm{O}) = 0.72$, $X(^{20}\mathrm{Ne}) = 0.25$, $X(^{24}\mathrm{Mg}) = 0.03$, central density $\rho_{\rm th} = 4.5 \times 10^9\ \mathrm{g\,cm^{-3}}$ and a range of central temperatures from 10^7 to 10^9 K. We used the EoS of Pols et al. (1995), assuming full ionization (i.e. we discarded the ionization pressure term). Note that neglecting the Coulomb corrections in the equation of state would increase the total mass by $3.79 \times 10^{-2}\,\mathrm{M_\odot}$ for our reference composition.

We integrated the general relativistic (GR) equations of hydrostatic equilibrium out from the centre

$$\frac{\mathrm{d}P}{\mathrm{d}r} = -\frac{Gm\rho}{r^2}\left(1+\frac{P}{\rho c^2}\right)\left(1+\frac{4\pi r^3 P}{mc^2}\right)\left(1-\frac{2Gm}{rc^2}\right)^{-1}, \tag{1}$$

where

$$\frac{\mathrm{d}m}{\mathrm{d}r} = 4\pi\rho r^2, \tag{2}$$

and

$$\frac{\mathrm{d}A}{\mathrm{d}r} = 4\pi n_{\rm b} r^2 \left(1-\frac{2Gm}{rc^2}\right)^{-\frac{1}{2}}. \tag{3}$$

Here m and A are the gravitational mass and baryon number enclosed within a sphere of radius r; ρ is the density, including contributions from both the rest mass and the thermal energy; $n_{\rm b}$ is the baryon number density. Rather than talking in terms of the baryon number A, which is a rather abstract quantity, it is convenient to convert this into a mass by multiplying by the atomic mass unit ($931.50\ \mathrm{MeV\,c^{-2}}$), and we refer to this quantity as the *baryonic mass*. If we had ignored the GR corrections, our estimate of the baryonic mass would have been increased by $1.30 \times 10^{-2}\,\mathrm{M_\odot}$ ($\sim$1 per cent). This difference is larger than what might have been expected; the reason, however, is analogous to that for the large difference between the Newtonian and the GR values for the maximum mass of a neutron star (Oppenheimer & Volkoff 1939).

To check the validity of our procedure, we computed a model without the GR corrections to reproduce the case considered by Miyaji & Nomoto (1987) and Nomoto (1987), where they used a composition $X(^{16}\mathrm{O}) = 0.12$, $X(^{20}\mathrm{Ne}) = 0.76$, $X(^{24}\mathrm{Mg}) = 0.12$, central density $3.98 \times 10^9\ \mathrm{g\,cm^{-3}}$ and central temperature $\log(T_{\rm c}) = 8.61$. We find a total mass $m = 1.3754\,\mathrm{M_\odot}$, which is very close to their published value of $1.375\,\mathrm{M_\odot}$.

This composition is, however, no longer considered appropriate since the reaction rate $^{12}\mathrm{C}(\alpha,\gamma)^{16}\mathrm{O}$ has been revised upwards (Dominguez, Tornambe & Isern 1993). This leads to a lower Ne and Mg abundance and a higher O abundance at the end of C burning than computed with the Fowler, Caughlan & Zimmerman (1975) rates (as was done in Miyaji & Nomoto 1987). To estimate the uncertainties introduced by these composition uncertainties, we investigated several different compositions found in the literature (Dominguez, Tornambe & Isern 1993; Gutiérrez et al. 1996; Ritossa, García-Berro & Iben 1996; Gil-Pons & García-Berro 2001) after the revision of the $^{12}\mathrm{C}(\alpha,\gamma)^{16}\mathrm{O}$ rate. The composition is important in determining the Coulomb parameter and $Y_{\rm e}$, and hence the magnitude of the Coulomb corrections. We used our reference model to give a lower bound on the critical mass (solid curve in Fig. 2) and the composition $X(^{16}\mathrm{O}) = 0.56$, $X(^{20}\mathrm{Ne}) = 0.29$, $X(^{24}\mathrm{Mg}) = 0.06$, $X(^{23}\mathrm{Na}) = 0.07$ and $X(^{12}\mathrm{C}) = 0.01$, which mimics the composition of Gil-Pons & García-Berro (2001) and has the lowest Coulomb correction to give an upper bound to the critical mass (dashed curve in Fig. 2).

Finally, we changed the threshold density $\rho_{\rm th}$ from 4.5×10^9 to $4 \times 10^9\ \mathrm{g\,cm^{-3}}$ in order to estimate the effect of the shift in the

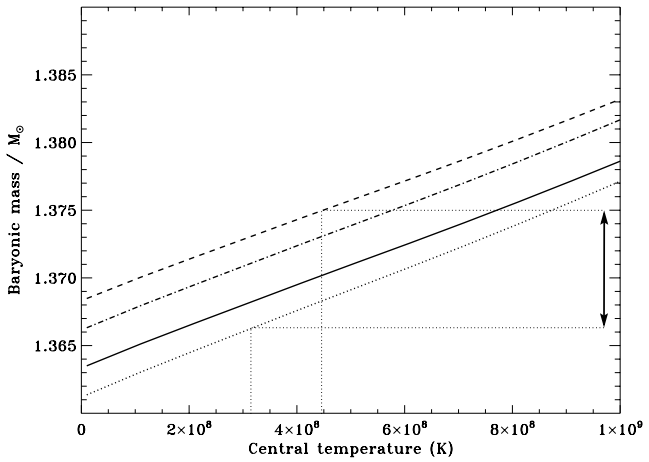

Figure 2. Baryonic mass versus central temperature for various ONeMg cores in hydrostatic equilibrium. Solid curve: reference model with $\rho_{\rm th} = 4.5 \times 10^9$ g cm $^{-3}$ with O and Ne mass fractions $X(^{16}{\rm O}) = 0.72$ and $X(^{20}{\rm Ne}) = 0.25$ (minimum mass for the variation in composition). Dashed curve: similar but with $X(^{16}{\rm O}) = 0.56$ and $X(^{20}{\rm Ne}) = 0.29$ (maximum mass for the variation in composition). Dotted curve: $\rho_{\rm th}$ is decreased to 4×10^9 g cm $^{-3}$ with the composition of the reference model. Dot-dashed curve: same model as for the dashed curve but with decreased $\rho_{\rm th}$. The thin dotted lines give the most likely range of parameters at the time of core collapse.

critical density due to the Coulomb corrections (the latter is the appropriate density without any Coulomb corrections; see Gutiérrez et al. 1996 for a detailed discussion). This change decreases the critical mass by 2×10^{-3} M$_\odot$ (dotted and dot-dashed lines in Fig. 2).

In the previous studies, the central temperature after the onset of e-captures ranged from $\log T_{\rm c} = 8.5$ to 8.65. For this temperature range, Fig. 2 then implies that the baryonic mass of the pre-collapse core should lie between 1.366 and 1.375 M$_\odot$ (the thin dotted curves) taking into account the uncertainties in temperature and composition. On the assumption that the loss of material during the formation of the neutron star is negligible, this then gives the predicted range for the baryonic mass of the neutron star (which we refer to as M_0).

3.1 Caveats

At this point, several caveats should be made about other effects that may systematically affect this estimate. First, we take the baryonic mass of the pre-collapse ONeMg core to be the same as that of the neutron star, neglecting any loss of material during the formation of the neutron star. In practice, some material may be ejected in the SN in a neutrino-driven wind (Quian & Woosley 1996). However, because of the steep density gradient at the edge of the ONeMg core, we expect this mass loss to be small, probably less than a few $\times 10^{-3}$ M$_\odot$, although it could potentially be as large as 10^{-2} M$_\odot$ and the amount of mass loss itself depends on the EoS (Janka, private communication). Secondly, an e-capture SN may occur between carbon shell flashes when the central density increases significantly (although we note that this point is not yet fully resolved). Because of the discrete nature of the carbon flashes, this may introduce a natural variation in the critical mass from star to star because of the variations of the thermal profile in the outer ONeMg core. In this context, we note that the assumption of an isentropic profile is unlikely to be correct in the outer parts of the ONeMg core.

It is clear that these effects could significantly change our estimate for the baryonic mass of the neutron star (probably decreasing it) and therefore our present estimates should only be considered as preliminary. However, with the expected progress in simulating e-capture SNe and calculating the evolution of their progenitors (with improved e-capture rates, a richer nuclear network, inclusion of accurate Coulomb corrections and using GR), we estimate that ultimately one should be able to pinpoint the mass of the collapsing core to within $\sim 2 \times 10^{-3}$ M$_\odot$.

4 CONSTRAINTS ON THE EQUATION OF STATE

On the hypothesis that the scenario presented in the previous sections is correct, we can use the information about the gravitational and baryonic masses of Pulsar B to place constraints on the EoS of neutron star matter. These turn out to be quite interesting.

For any given EoS for neutron star matter, one can calculate the relation between the gravitational mass and the baryonic mass (bearing in mind that the rotation speed is so low that taking the object to be spherical and non-rotating is an excellent approximation). The present gravitational mass (known from observations) and the baryonic mass (known from the stellar evolution calculations) then define an error box through which the relations calculated from the EoSs would need to pass in order to be consistent. In this section, we discuss how the constraints obtained in this way turn out. The observed gravitational mass ($M_{\rm G} = 1.249 \pm 0.001$ M$_\odot$) and the calculated baryonic mass (M_0 in the range 1.366–1.375 M$_\odot$) specify the boundaries of the error box.

Results obtained by integrating the GR equations of hydrostatic equilibrium (equations 1–3) for a range of EoSs are shown in the four panels of Fig. 3, each corresponding to a particular class of EoSs (we use a modified form of the classification in the paper by Morrison et al. 2004). All of these EoSs give the maximum gravitational mass $M_{\rm max}$ for a non-rotating neutron star as being above 1.5 M$_\odot$, in line with observations. Class I EoSs (top-left panel) come from non-relativistic many-body calculations with 'realistic' potentials: APR98 (Akmal, Pandharipande & Ravenhall 1998), WFF88 (Wiringa, Fiks & Fabrocini 1988) and FPS (Lorenz, Ravenhall & Pethick 1993) include only nucleonic degrees of freedom; BJ74 (Bethe & Johnson 1974) and MOSZ74 (Mozskowski 1974) include also hyperonic components at the higher densities. Class II EoSs (top-right panel) use relativistic mean-field (or effective-field) approximations including hyperonic degrees of freedom: GLEN240 and GLEN300 (Glendenning 2000), HOF01 (Hofmann, Keil & Lenske 2001). We also include here one EoS representing a hybrid stellar model (nucleons + quarks): GLENHYB (Glendenning 2000). Class III EoSs (bottom-left panel) use non-relativistic phenomenological potentials of the Skyrme type (see Stone et al. 2003 and references therein). Class IV EoSs (lower-right panel) are for other phenomenological non-relativistic potentials: BPAL21 and BPAL31 (Prakash et al. 1997) have only nucleonic degrees of freedom, while BAL97 (Balberg & Gal 1997) includes hyperons at high density. All of these high-density EoSs were joined on to the Baym–Bethe–Pethick EoS (Baym, Bethe & Pethick 1971) at a density of $\sim 1.4 \times 10^{14}$ g cm^{-3} (0.08–0.09 fm^{-3}) and, in turn, this was joined on to the Baym–Pethick–Sutherland EoS (Baym, Pethick & Sutherland 1971) at 4.2×10^{11} g cm^{-3} (2.5×10^{-4} fm^{-3}). By doing this, the inner and outer crust of the neutron star were treated in the same way for all of the EoSs, and so all of the differences seen result from differences in the treatment of the high-density matter.

The most clear-cut result is that none of the class II models tested in this work gives predictions in line with our constraint. For the other classes (I, III and IV), the situation is less clear and depends on the particular properties of each individual EoS. For the

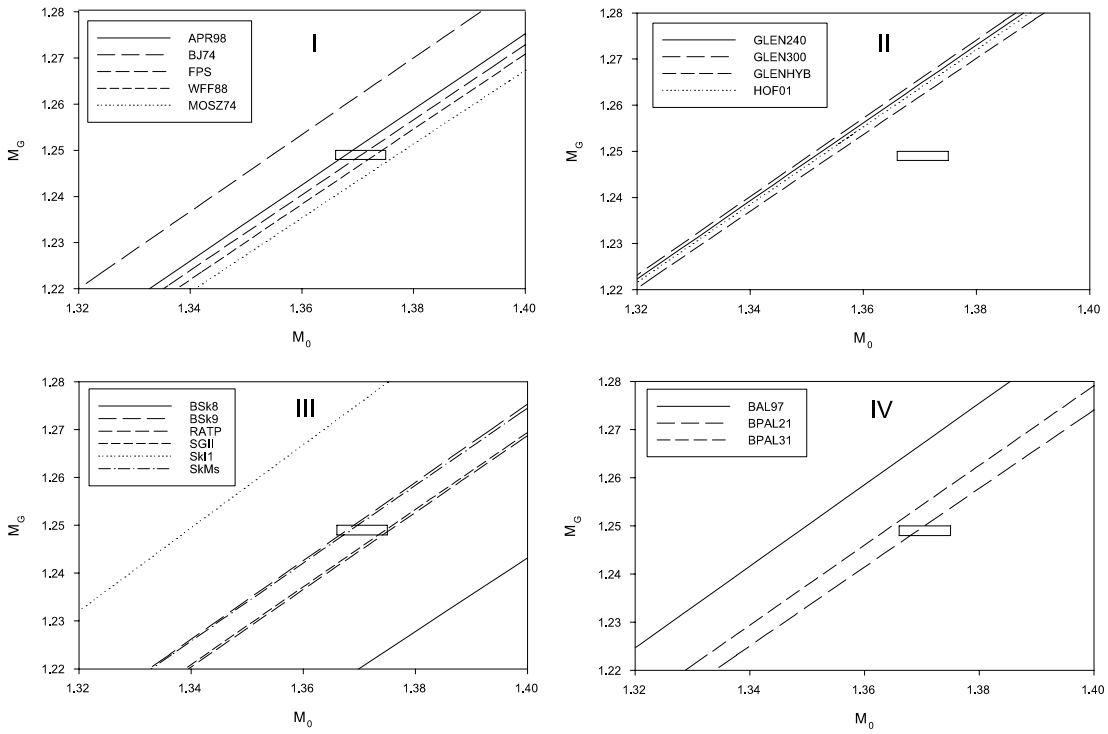

Figure 3. Relation between the gravitational mass $M_{\rm G}$ of neutron star models and their baryonic mass M_0, measured in units of the solar mass $\mathrm{M}_\odot$, for various EoSs. The constraint derived in this paper is marked by a rectangle. For more explanation, see text.

phenomenological Skyrme potentials, the EoSs give a wide range of predictions within the region delimited by SkI1 and BSk8. Those parametrizations giving $M_{\rm G}/M_0$ curves passing through the error box give $M_{\rm max}$ between 1.6 and 1.9 $\mathrm{M}_\odot$. All of those for which $M_{\rm max} > 1.9\,\mathrm{M}_\odot$ give curves passing above the error box, while those for which $M_{\rm max} < 1.6\,\mathrm{M}_\odot$ give curves passing below it. With reference to the discussion in Stone et al. (2003) and using the notation of that paper, we note that all of the Skyrme EoSs passing through the error box are type II parametrizations whereas all of those coming from type I parametrizations pass above it.

Apart from the comments made above, there is no simple general interpretation of the implications of our constraint for the physics behind the particular EoSs. It is important to recognize that our constraint (assuming that our overall scenario is correct) represents a necessary but not sufficient condition for choosing a suitable EoS for neutron star models. Additional observational information is needed, in particular concerning the neutron star maximum mass which, in combination with the present constraint, would give a more definitive criterion for the choice of physical model for the EoS. Also, the influence of different treatments for the inner and outer crust needs to be investigated before any final conclusion is drawn.

5 CONCLUSIONS

In this paper, we have demonstrated that the measured gravitational mass of Pulsar B in the double pulsar J0737–3039 can be used to give a new test of the neutron star EoS if one makes the all-important assumption that Pulsar B was formed in an e-capture SN. In this case, its baryonic mass can be estimated theoretically, and comparison between this and its gravitational mass can then be used to constrain the EoS. We have reconstructed the possible evolutionary histories for J0737–3039 in the main formation channels to support the hypothesis of Pulsar B having originated in an e-capture SN and have discussed possible tests of this hypothesis. Future refinements, both of the stellar evolution models (to better pin down the critical pre-collapse mass) and of e-capture collapse models (to quantify the possible mass loss) should lead to a more stringent constraint which, when combined with other astrophysical EoS constraints, can provide new insight into the physics of neutron star matter.

ACKNOWLEDGMENTS

We thank H.-Th. Janka and M. Kramer for very useful discussions and for sharing the results of some of their unpublished work, and C. M. Keil for supplying numerical data for EoS HOF 01 in Fig. 3. This work was in part supported by a European Research & Training Network on Type Ia Supernovae (HPRN-CT-20002-00303, PhP, PL), a Talent Fellowship (JDMD) from the Netherlands Organization for Scientific Research (NWO), EPSRC Grant 02300018 (WGN), an Advanced Computing Grant from US DOE Scientific Discovery (JRS) and US DOE grant DE-FG02-94ER40834 (JRS).

REFERENCES

Akmal A., Pandharipande V. R., Ravenhall D. G., 1998, Phys. Rev., C58, 1804
Arons J., Backer D. C., Spitkovsky A., Kaspi V. M., 2005, in Rasio F. A., Stairs I. H., eds, Binary Radio Pulsars, in press (astro-ph/0404159)
Balberg S., Gal A., 1997, Nucl. Phys., A625, 435
Baym G., Bethe H. A., Pethick C., 1971, Nucl. Phys., A175, 225
Baym G., Pethick C., Sutherland P., 1971, ApJ, 170, 299
Bethe H. A., Johnson M., 1974, Nucl. Phys., A230, 1
Bhattacharya D., van den Heuvel E. P. J., 1991, Phys. Rep., 203, 1
Brown G. E., 1995, ApJ, 440, 270
Burgay M. et al., 2003, Nat, 426, 531
Chevalier R. A., 1993, ApJ, 411, L33

Coles W. A., McLaughlin M. A., Rickett B. J., Lyne A. G., Bhat N. D. R., 2005, ApJ, 623, 392
Dewi J. D. M., Pols O. R., 2003, MNRAS, 344, 269
Dewi J. D. M., van den Heuvel E. P. J., 2004, MNRAS 349, 169
Dewi J. D. M., van den Heuvel E. P. J., 2005, in Rasio F. A., Stairs I. H., eds, Binary Radio Pulsars, in press
Dewi J. D. M., Pols O. R., Savonije G. J., van den Heuvel E. P. J., 2002, MNRAS, 331, 1027
Dominguez I., Tornambe A., Isern J., 1993, ApJ, 419, 268
Fowler W. A., Caughlan G. R., Zimmerman B. A., 1975, ARA&A, 13, 69
Gil-Pons P., García-Berro E., 2001, A&A, 375, 87
Glendenning N. K., 2000, Compact Stars. Springer, Berlin
Gutiérrez J., García-Berro E., Iben I., Jr, Isern J., Labay J., Canal R., 1996, ApJ, 459, 701
Habets G. M. H. J., 1986, A&A, 167, 61
Hofmann F., Keil C. M., Lenske H., 2001, Phys. Rev., C64, 025804
Ivanova N., Belczynski K., Kalogera V., Rasio F. A., Taam R. E., 2003, ApJ, 592, 475
Kramer M. et al., 2005, in press (astro-ph/0503386)
Lorenz C. P., Ravenhall D. G., Pethick C. J., 1993, Phys. Rev. Lett., 70, 379
Lyne A. G. et al., 2004, Sci, 303, 1153
Manchester R. N. et al., 2005, ApJ, 621, L49
Miyaji S., Nomoto K., 1987, ApJ, 318, 307
Miyaji S., Nomoto K., Yokoi K., Sugimoto D., 1980, PASJ, 32, 303
Morrison I. A., Baumgarte T. W., Shapiro S. L., Pandharipande V. R., 2004, ApJ, 617, 135
Mozskowski S., 1974, Phys. Rev. D, 9, 1613
Nomoto K., 1984, ApJ, 277, 791
Nomoto K., 1987, ApJ, 322, 206
Oppenheimer J. R., Volkoff G. M., 1939, Phys. Rev., 55, 374
Podsiadlowski Ph., Langer N., Poelarends A. J. T., Rappaport S., Pfahl E., 2004, ApJ, 612, 1044
Pols O. R., Tout C. A., Eggleton P. P., Han Z., 1995, MNRAS, 274, 964
Prakash M., Bombaci I., Prakash M., Lattimer J. M., Ellis P. J., Knorren R., 1997, Phys. Rep., 280, 1
Quian Y.-Z., Woosley S. E., 1996, ApJ, 471, 331
Ransom S. M., Kaspi V. M., Ramachandran R., Demorest P., Backer D. C., Pfahl E. D., Ghigo F. D., Kaplon D. L., 2004, ApJ, 609, 71
Ritossa C., García-Berro E., Iben I., Jr, 1996, ApJ, 460, 489
Scheck L., Plewa T., Janka H.-Th., Kifonidis K., Müller E., 2004, Phys. Rev. Lett., 92, 1103
Stone J. R., Miller J. C., Koncewicz R., Stevenson P. D., Strayer M. R., 2003, Phys. Rev., C68, 034324
Willems B., Kalogera V., 2004, ApJ, 603, L101
Willems B., Kalogera V., Henninger M., 2004, ApJ, 616, 414
Wiringa R. B., Fiks V., Fabrocini A., 1988, Phys. Rev., C38, 1010
Woosley S. E., Heger A., Weaver T. A., 2002, Rev. Mod. Phys., 74, 1015

This paper has been typeset from a TEX/LATEX file prepared by the author.